The Effect of Trailing Edge Grid Resolution in Large-Eddy Simulations

Kenji Miki[1], Ali Ameri[1,2]

[1] NASA Glenn Research Center, [2] The Ohio State University

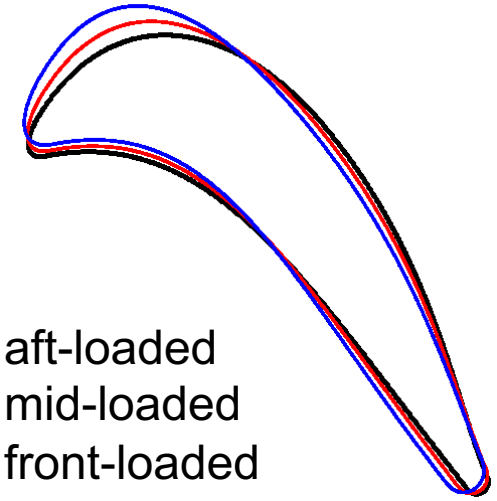
ASME Turbo Expo 2023
Turbomachinery Technical Conference and Exposition
GT2023-102276
June 26-30, 2023, Boston, MA, USA

Outline

- Introduction
- Experimental Setup
- Numerical Setting
- Summary of Past Study (IGTI 2022-82335)
- Grid Resolution
- Results (20M and 50M mesh)
  - Instantaneous flow fields
  - Turbulent kinetic energy and dissipation function profiles
  - Shear stress and boundary layer profiles
  - Comparison with the experimental data
- Conclusions

Introduction and Motivation

Due to the complex fabrication process of CMC blades, larger blade trailing edge thicknesses and larger leading-edge radii of curvature are expected. These features significantly alter aerodynamic performance especially near the trailing edge and thus the loss profile.



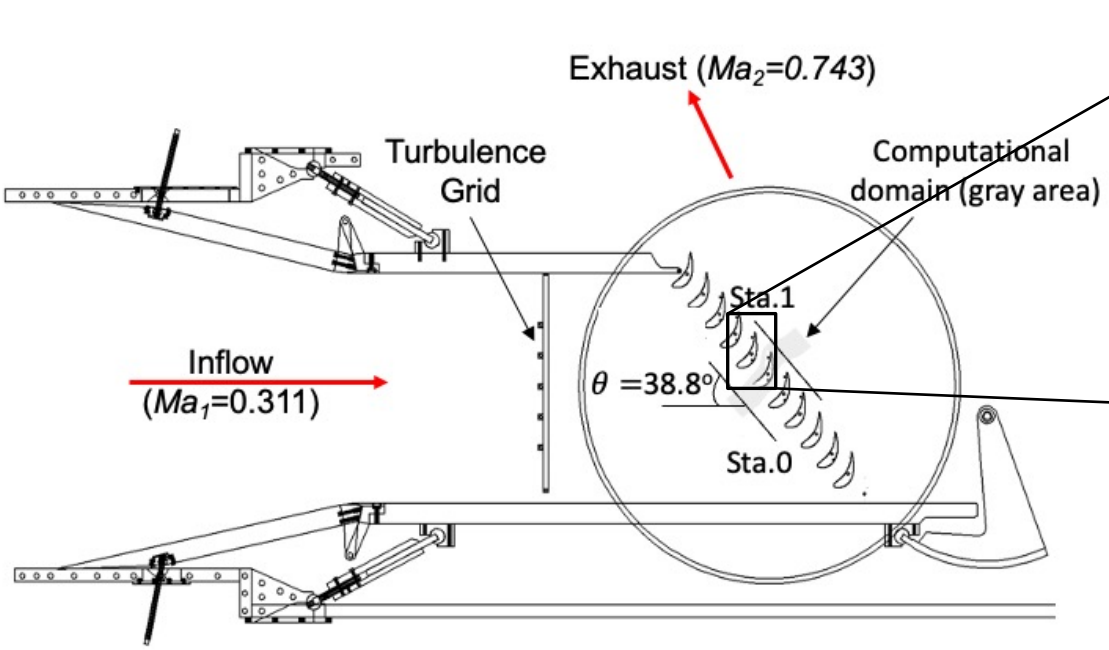
- aft-loaded
- mid-loaded
- front-loaded

CMC blade coordinates tested at NASA GRC [1]

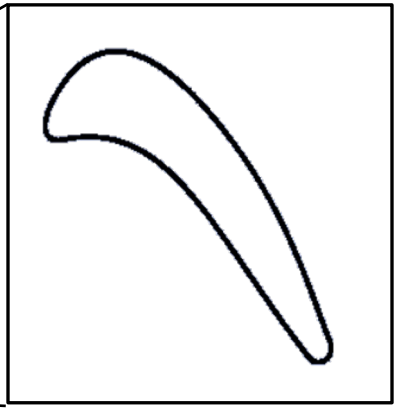
- Lyall, *et al*. [2], Keadle, *et al.* [3] and Arko-, *et al.* [4] used RANS to investigate the front- and aft-loaded designs at a relatively low free-stream turbulence (FST) (Tu~3.1-3.3%).
- Medic and Sharma [5] and Bolinches-Gisbert *et al.* [6] used LES to investigate the LPT blades with (Tu=4%) and without FST for 30,000 < Re < 150,000 and Re ~ 50,000,
- Pichler *et al.* [7] performed a grid convergence study for LPT DNS at a Re=60,000 with the aim of resolving the background turbulence with 18, 72 and 200 million points
- Miki and Ameri [8] performed LES with 20 million points (157,000 < Re < 314,000) and RANS for the CMC blades (Tu=10~13%) and compared the results against the data by Giel *et al.* [1]

Large Eddy Simulation (LES) shows some success to capture such characteristics of CMC blades [8]. However, there is still challenging issue such as a grid requirement.

NASA GRC Transonic Turbine Blade Facility



Front-loaded Blade (CMC9)

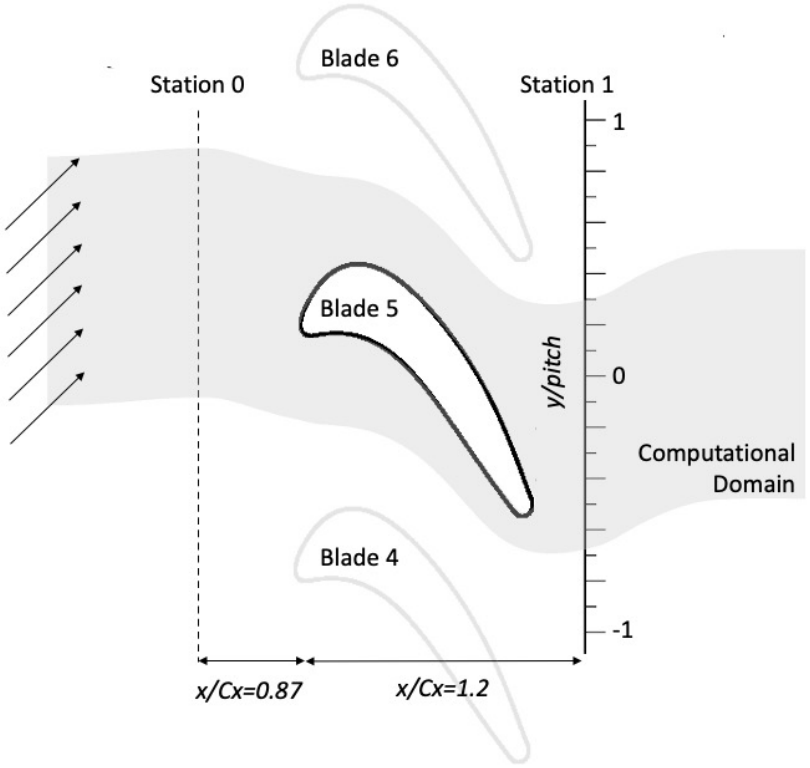


Geometry of Blade	Value
Leading Edge Diameter, [mm]	22.48
Trailing Edge Diameter, [mm]	11.68

	Test Condition
$T_{t,in}$ [K]	295.6
$P_{t,in}/P_{ex}$	1.442
Re_{ex}	314,500
M_{in}/Ma_{ex}	0.311/0.743
Tu [%]	13
Ts/C_x	0.02
β [deg.]	38.8
$\delta_{99}/(h/2)$	0.24

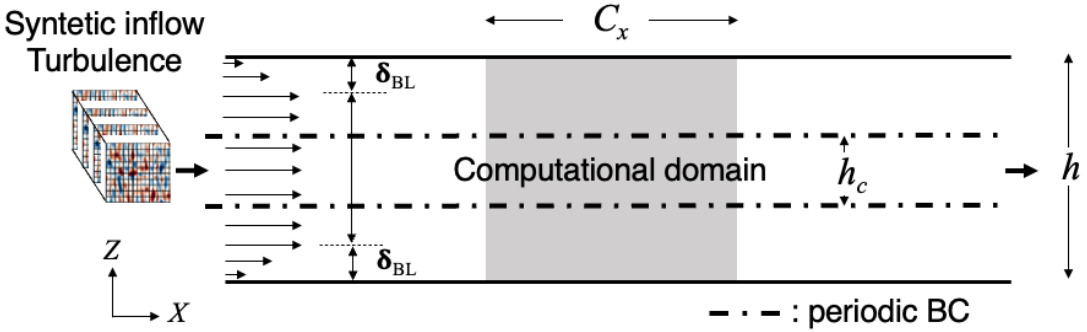
- Pressure loading and loss profiles were measured at Station 1.
- Turbulence grid, which is designed to generate isotropic turbulence, is located upstream (please note that the grid is not parallel to the blade row)
- Although BL thickness is ~25% of a half of blade span, the end wall effect could influence the flow field in the mid-span.

Glenn-HT and Numerical Setting



The in-house code, **Glenn-HT**, which has been continuously developed and validated over the past two decades at the NASA Glenn Research Center is used.

Features	Applications
Multi-block, structured, (U)RANS/LES (lots of turbulence models), flow-solid interactions, Implicit N-S solver	Turbine/compressor efficiency, Turbine cooling (conjugate heat transfer), heat exchanger performance, etc.

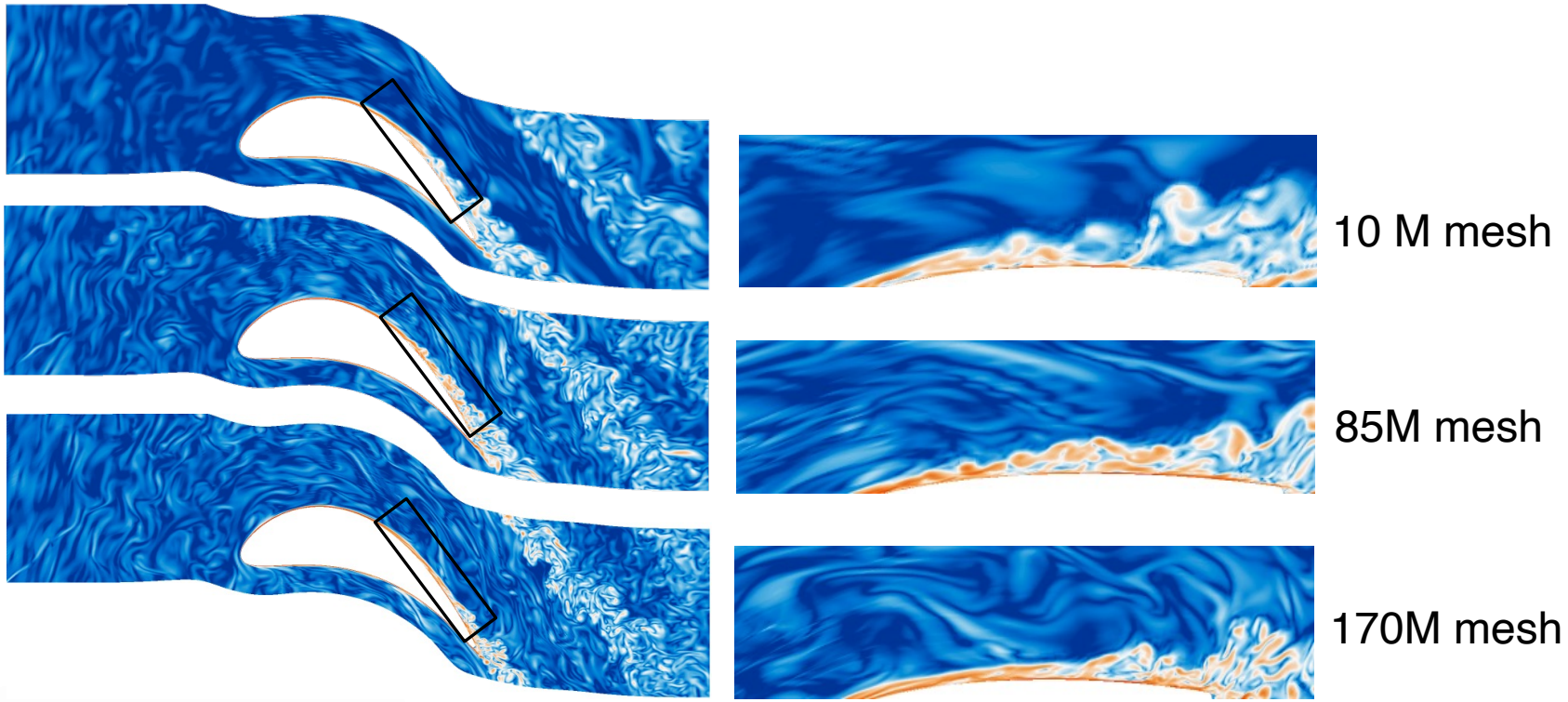


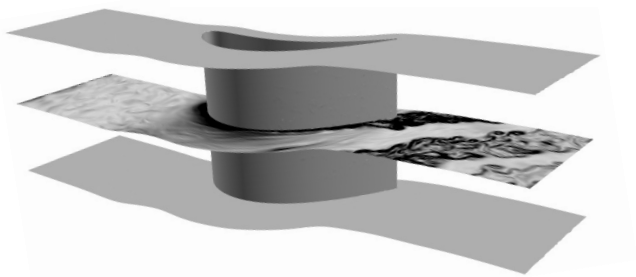
- Inflow turbulence is generated by Tu and Ts through the digital filtering approach [9].
- LES + localized dynamic *k*-equation model (LDKM) [10].
- AUSM$^+$-up with MUSCL is used for inviscid flux [11].

A LES mesh with adequate resolution is required for this quasi-2D problem.

Key Learning of Previous Grid Resolution Study

In our previous study [12], we simulated the variable Speed Power Turbine (VSPT) blade and performed grid sensitivity analysis.

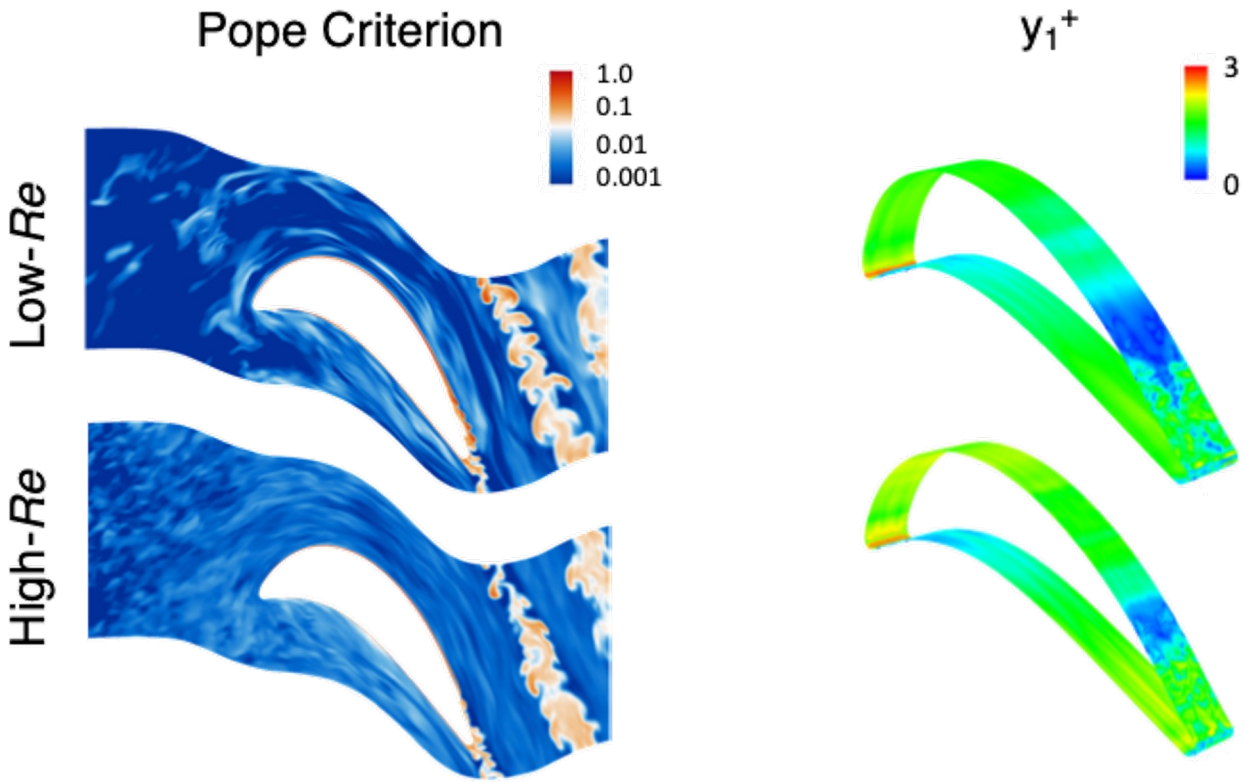




Full 3D simulation of VSPT

- The mechanism of the BL instability changes from separation, shear layer with K-H instability to Bypass transition as the grid resolution increases.
- 170 M mesh including the end wall was shown to be adequate for LES (Re ~220,000 and Tu=10-15%).
- Based on this, we generated 20 M mesh for the quasi-2D simulation (the end wall is not included) in [8].

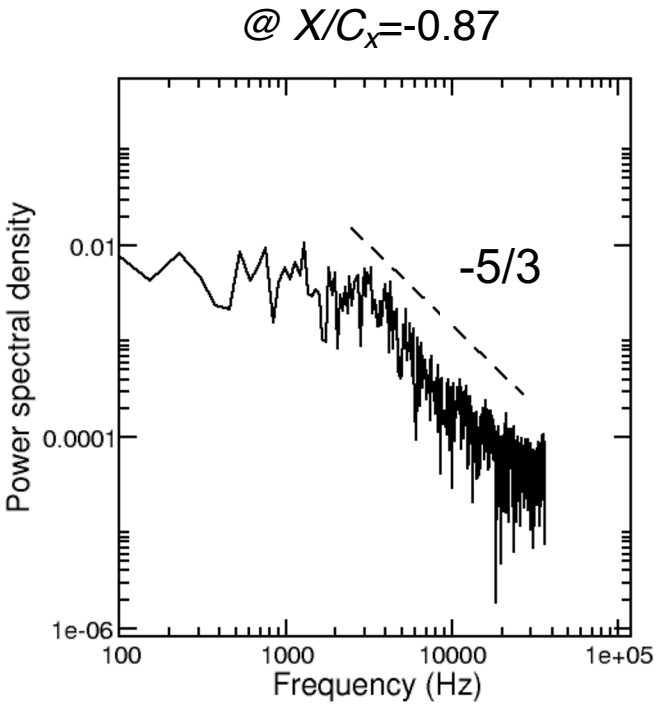
Grid Resolution Test (20M Mesh) [8]



- Pope Criterion is a good indicator to check whether the grid resolution in the freestream region adequately resolves the turbulence.
- Near the wall, we use very fine mesh (1.25×10^{-6} [m]) to resolve the BL and y^+_1 is ~1 for most of the surface including the suction side.
- In the midspan wall region, on the average, x^+_1 value is of ~10 and z^+_1 is of ~20.

The 20M mesh seemed to be satisfied with the conventional grid resolution requirements for LES.

Characteristics of Inflow Turbulence [8]



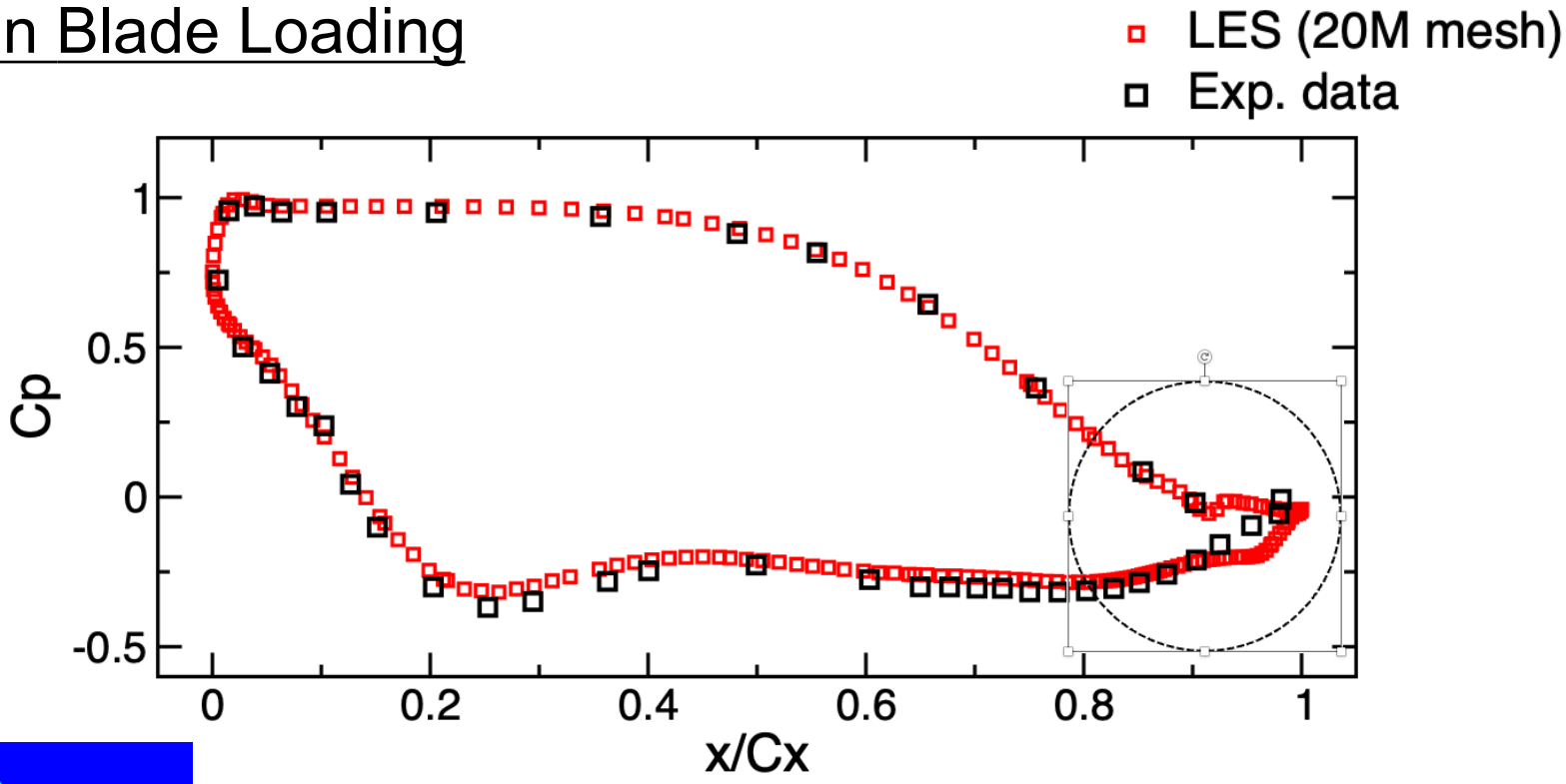
- The quality of incoming turbulence and LES are assessed by calculating the power spectral density of the normalized axial velocity component at $X/C_x = -0.87$.
- It is observed that the spectral slope follows the Kolmogorov -5/3 law.
- It is confirmed that u'_{rms}/U_0, v'_{rms}/U_0, and w'_{rms}/U_0 make up isotropic incoming turbulence in this setup and the cross-components ($u'v'$, $u'w'$, and $v'w'$) are almost zero.

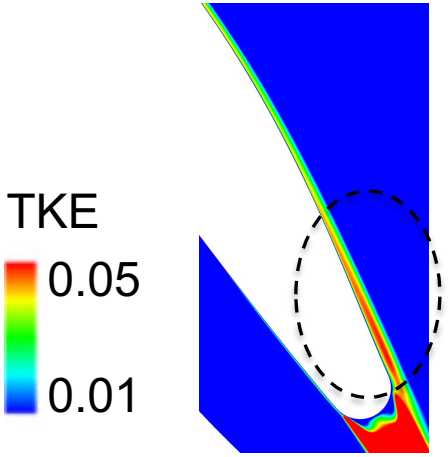
LES [8]					Exp. [13]	
$X/C_x = -0.87$					Station 0	
Tu [%]	u'_{rms}/U_0	v'_{rms}/U_0	w'_{rms}/U_0	$(u'v')^{1/2}/U_0$, $(u'w')^{1/2}/U_0$, $(v'w')^{1/2}/U_0$	Tu [%]	Pitch Variance [%]
11.0	0.06	0.07	0.06	< 0.001	12.4	± 2.6

A realistic inflow turbulence was modeled by using the current numerical setting and the 20M mesh.

Issues of the Previous Study [8]

Midspan Blade Loading



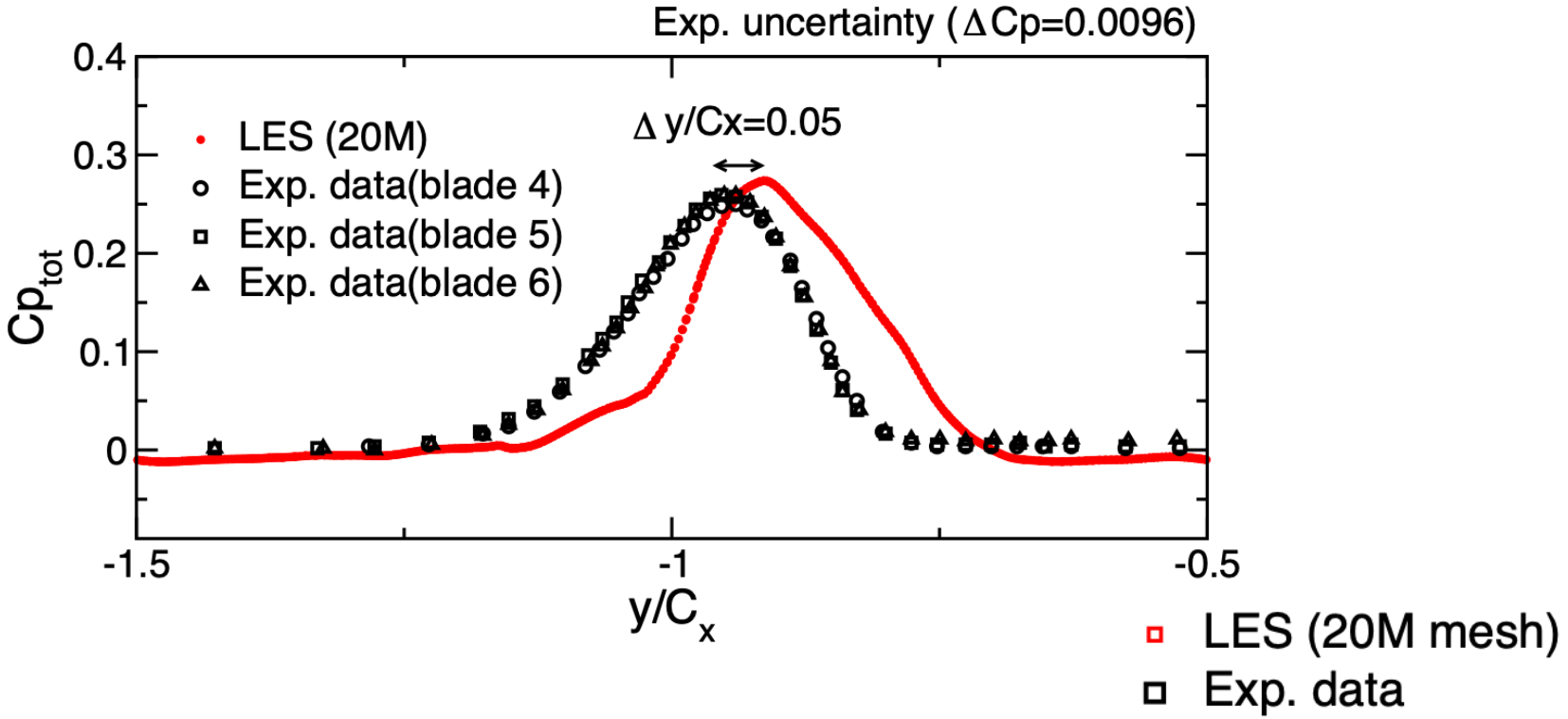


Turbulent Kinetic Energy

- Near the trailing edge, there is noticeable discrepancy in the blade loading.
- There is a sudden increase in the turbulent kinetic energy (TKE) profile, which indicates the separation on the suction side, which is not seen in the data

Issues of the Previous Study, con [8]

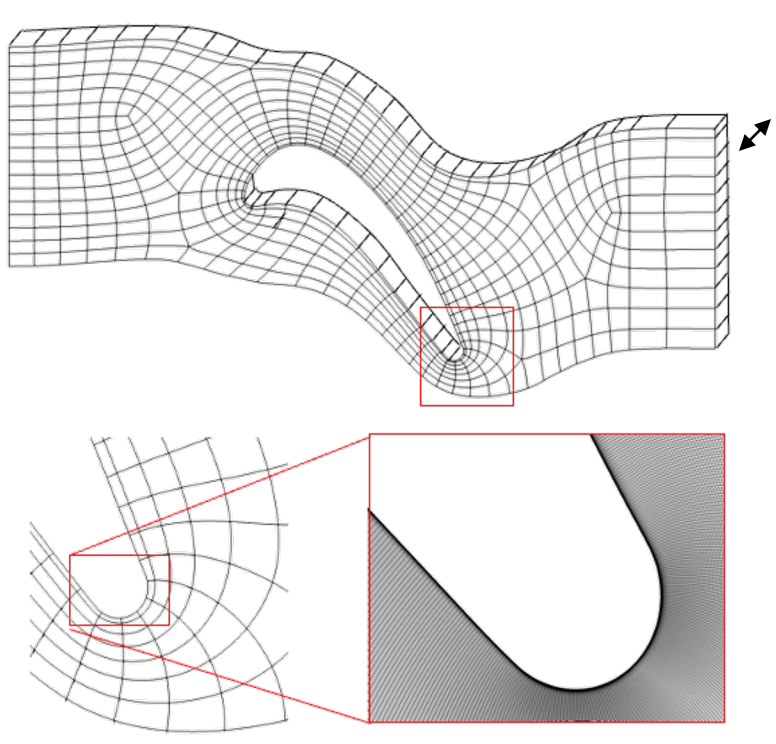
Wake Profile



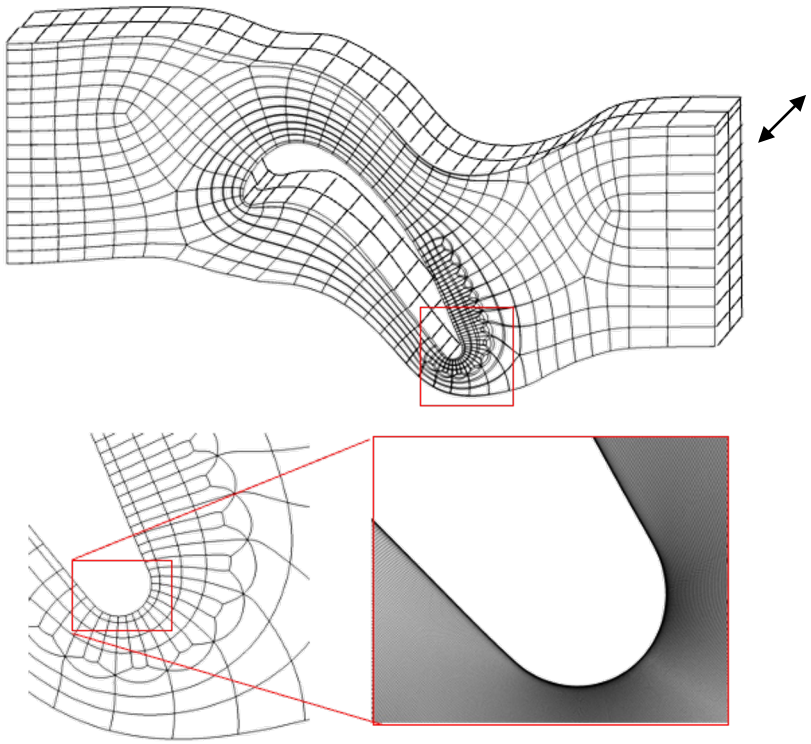
- The area-averaged kinetic energy loss is comparable to the data.
- However, there is a noticeable "shift" (~$\Delta y/Cx$=0.05) between the data and the predicted profiles.

Although the grid resolution (~20M) satisfies the conventional LES requirements, these results still need to be improved.

New Grid



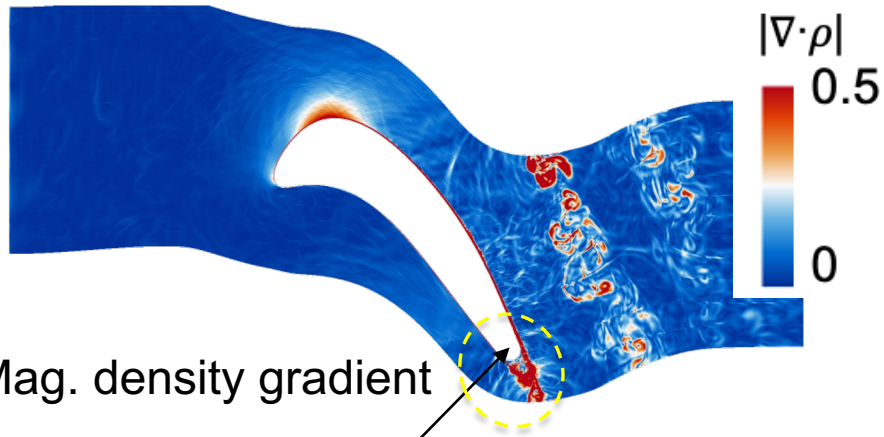
LES (20 M) grid [8]



LES (50M) grid (Current study)

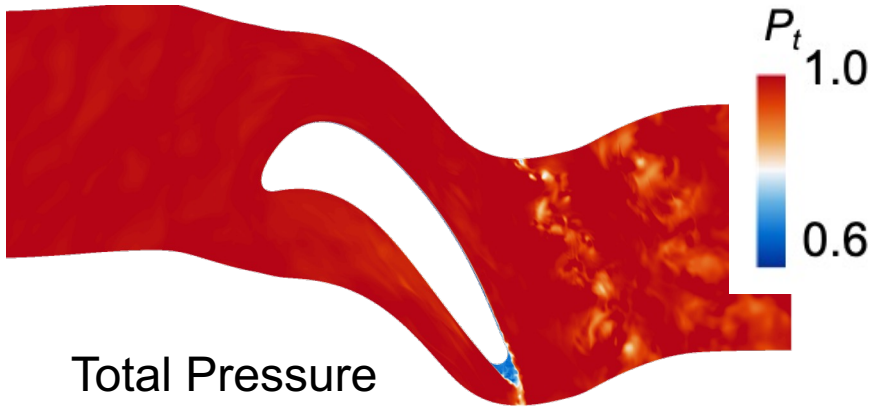
- In order to resolve these issues, we decided to improve the quality of mesh near the blade (the grid spacing near the wall and the grid topology/resolution in the upstream region are the same.)
- The span of the domain is $0.2 \times C_x$ and $0.3 \times C_x$, and the spanwise grid resolutions are 32 and 64 for the LES (20M) and LES (50M) meshes.
- Near the end of the suction side and the trailing edge, the grid resolution is increased for the LES (50M) grid by three folds compared to the LES (20M) grid.

Instantaneous Flow Fields

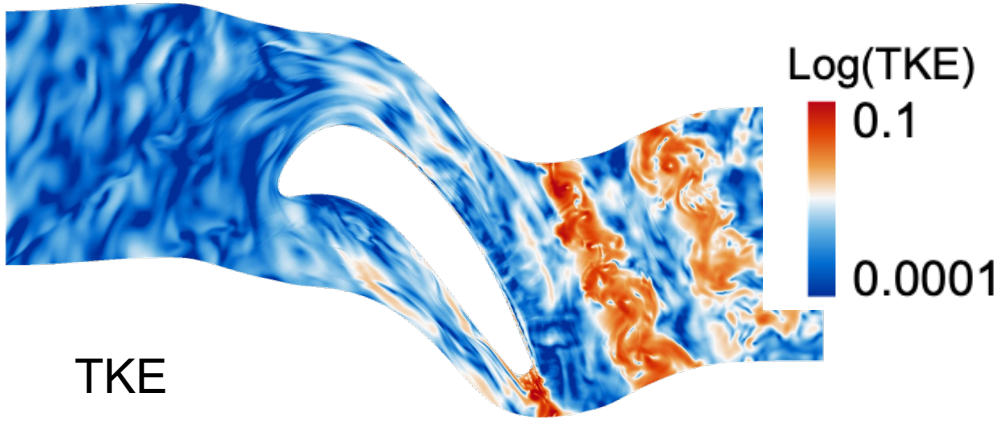


Mag. density gradient

Very stable



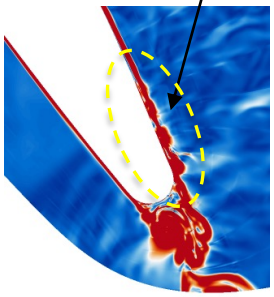
Total Pressure



TKE

Low Re=157,000 [8]

Wavy boundary layer

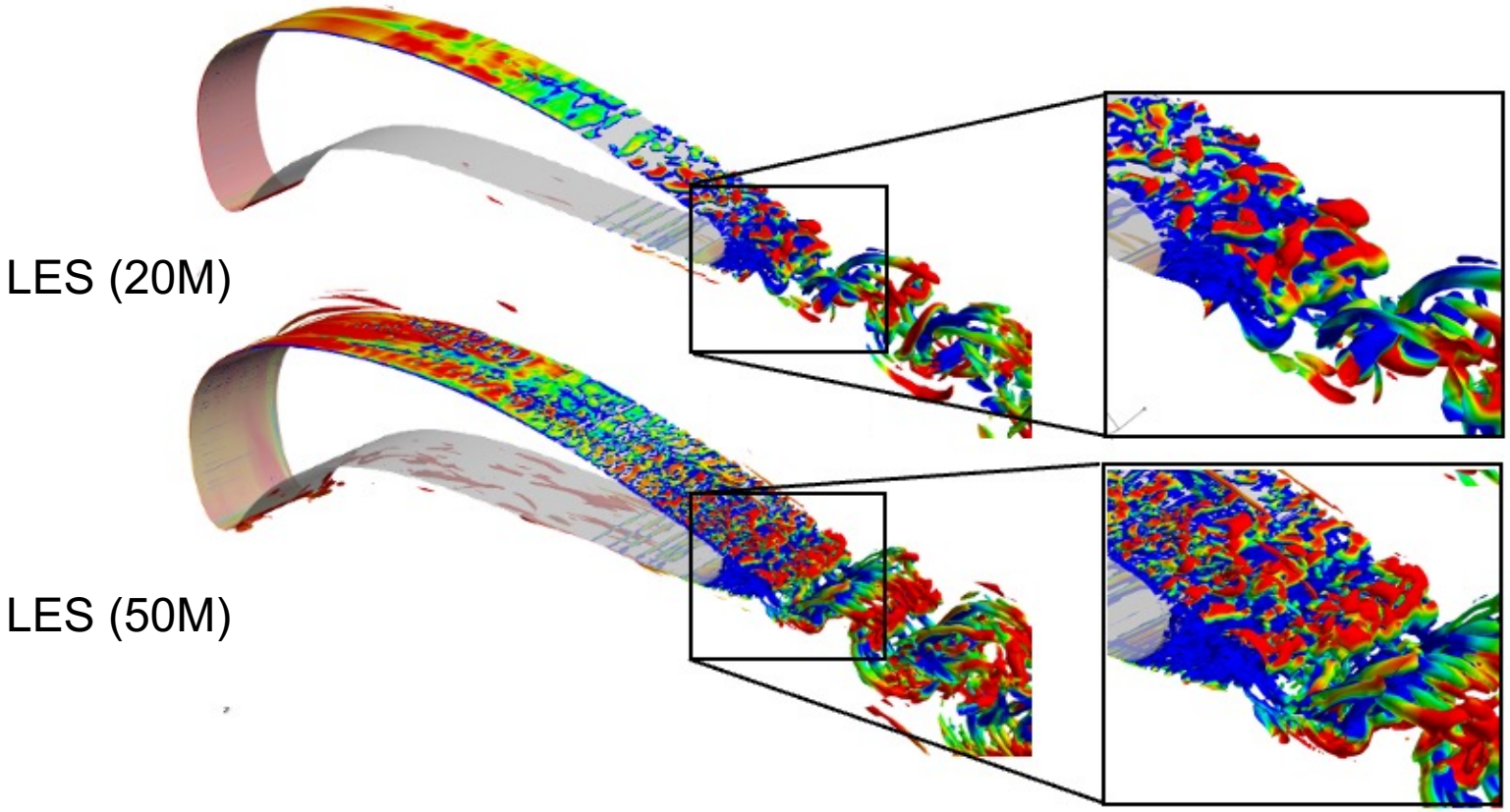


Mag. density gradient

- The small-scaled eddies generated at the inlet are propagated and elongated through the acceleration on the suction side.
- The boundary layer looks to be stable all along the suction side.
- With the large trailing edge diameter, a large recirculation zone is formed and stable (at a lower Re = 157,000, a large wavey oscillation is initiated, and recirculation zone is greatly disturbed)

3D Instantaneous Flow Fields

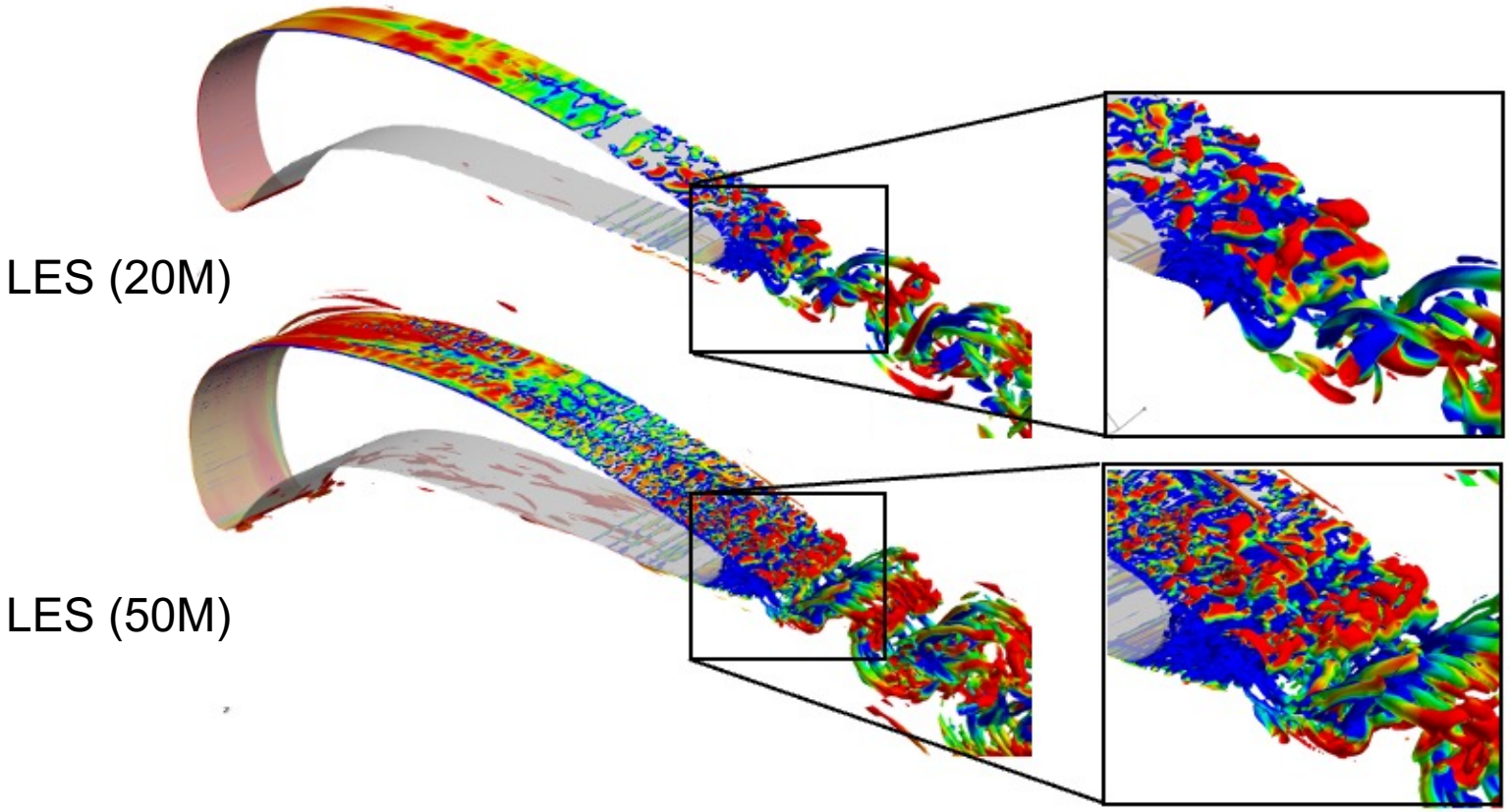
Contour-surfaces of Q-criterion (=1) colored by the total pressure



- Vortex roll-up near the trailing edge and the hairpin vortices are developed downstream, and then the Von Karman (V-K) vortices are formed.
- Using LES (50M) mesh, many more small-scaled structures are coupled with the large structures, and the small-scaled disturbances start developing further upstream and then break down near the trailing edge

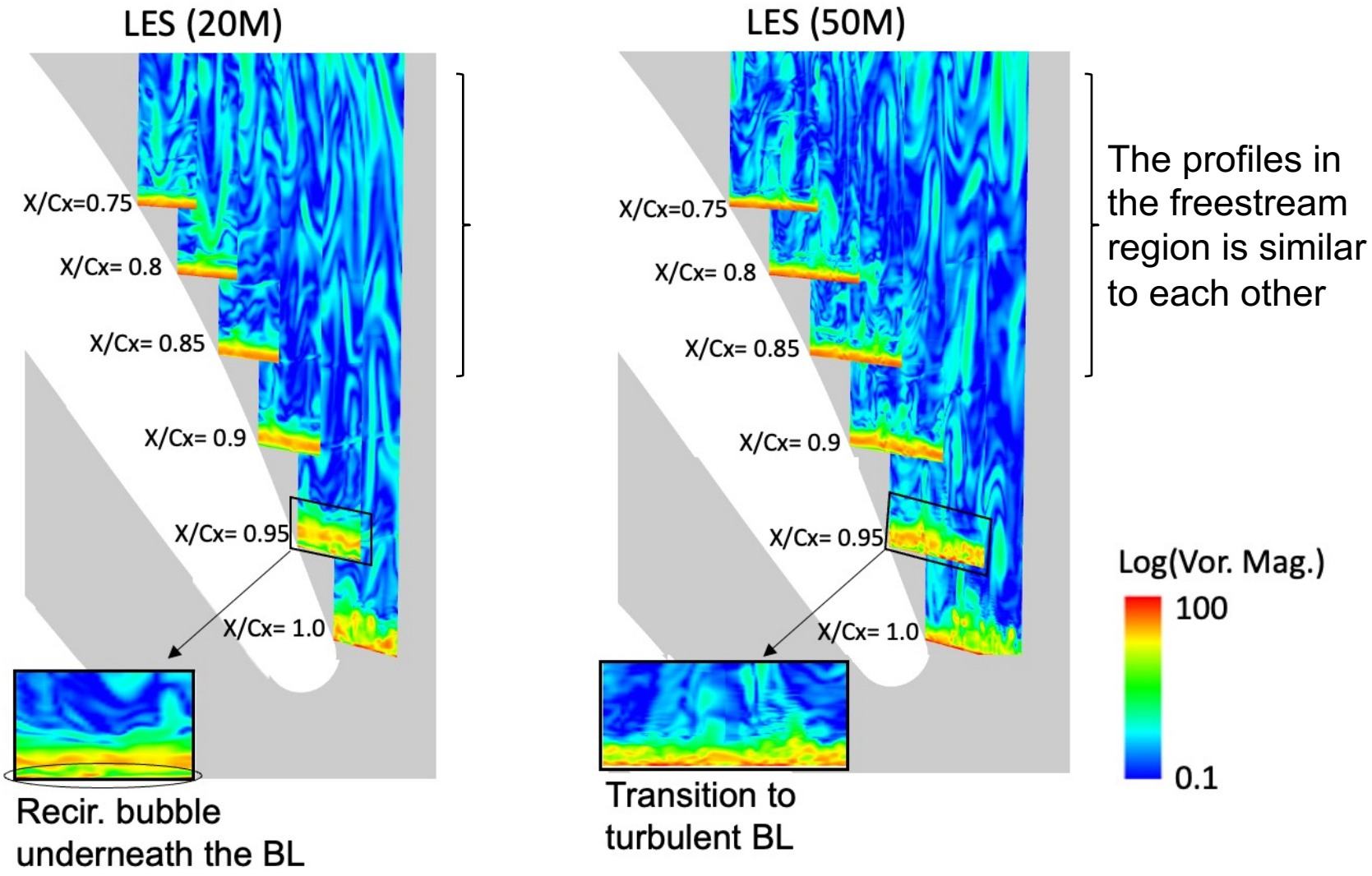
3D Instantaneous Flow Fields, con

Contour-surfaces of Q-criterion (=1) colored by the total pressure



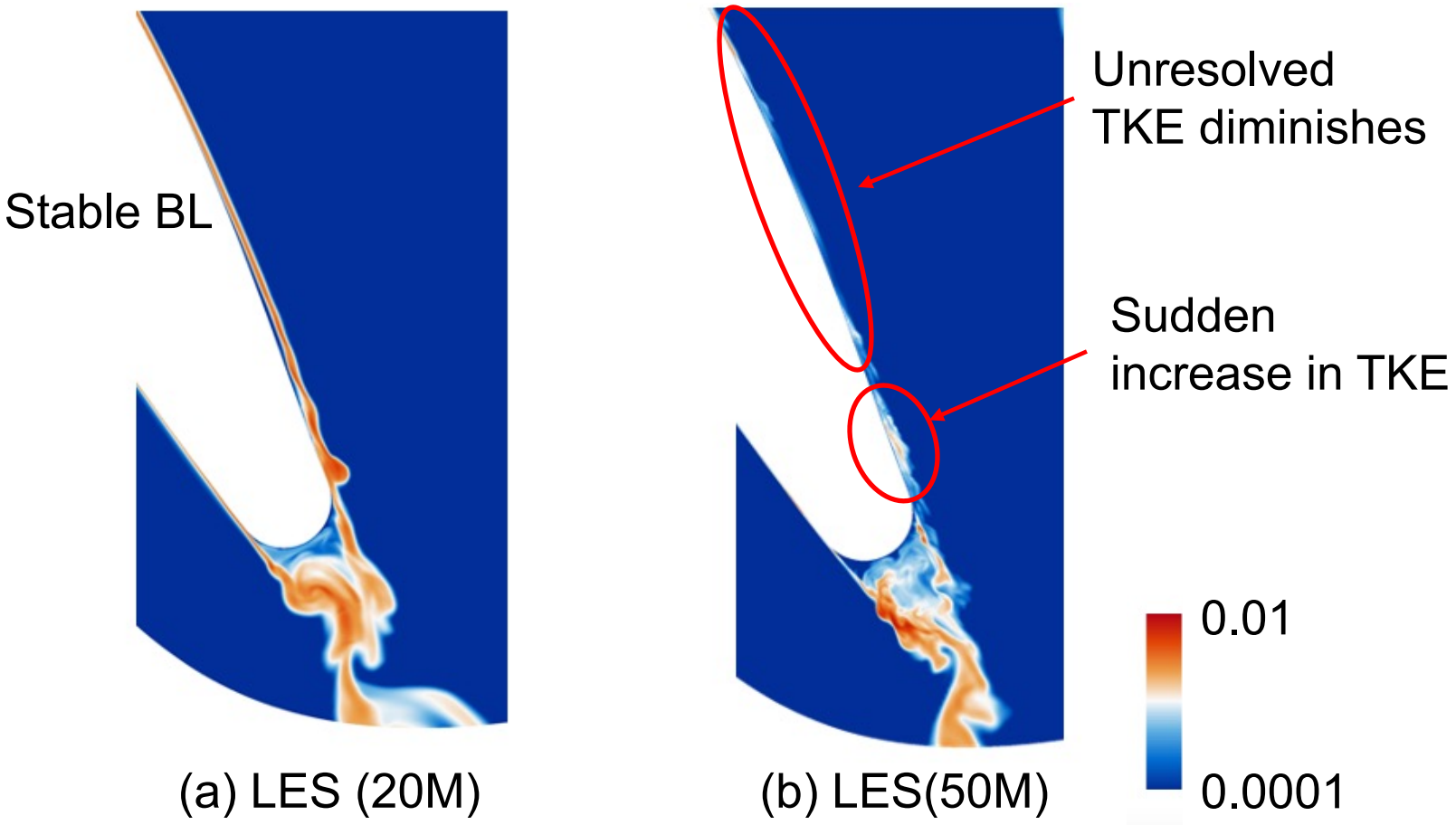
- This qualitatively confirms that bypass transition to the turbulent boundary layer takes place when the grid is further refined, and transition is not due to separation reattachment.
- The large eddy structure in the wake is quite two-dimensional and that the eddy size is not changed from the LES (20M) case -> No noticeable difference in the flow field in the spanwise direction

Contour of Vorticity Magnitude



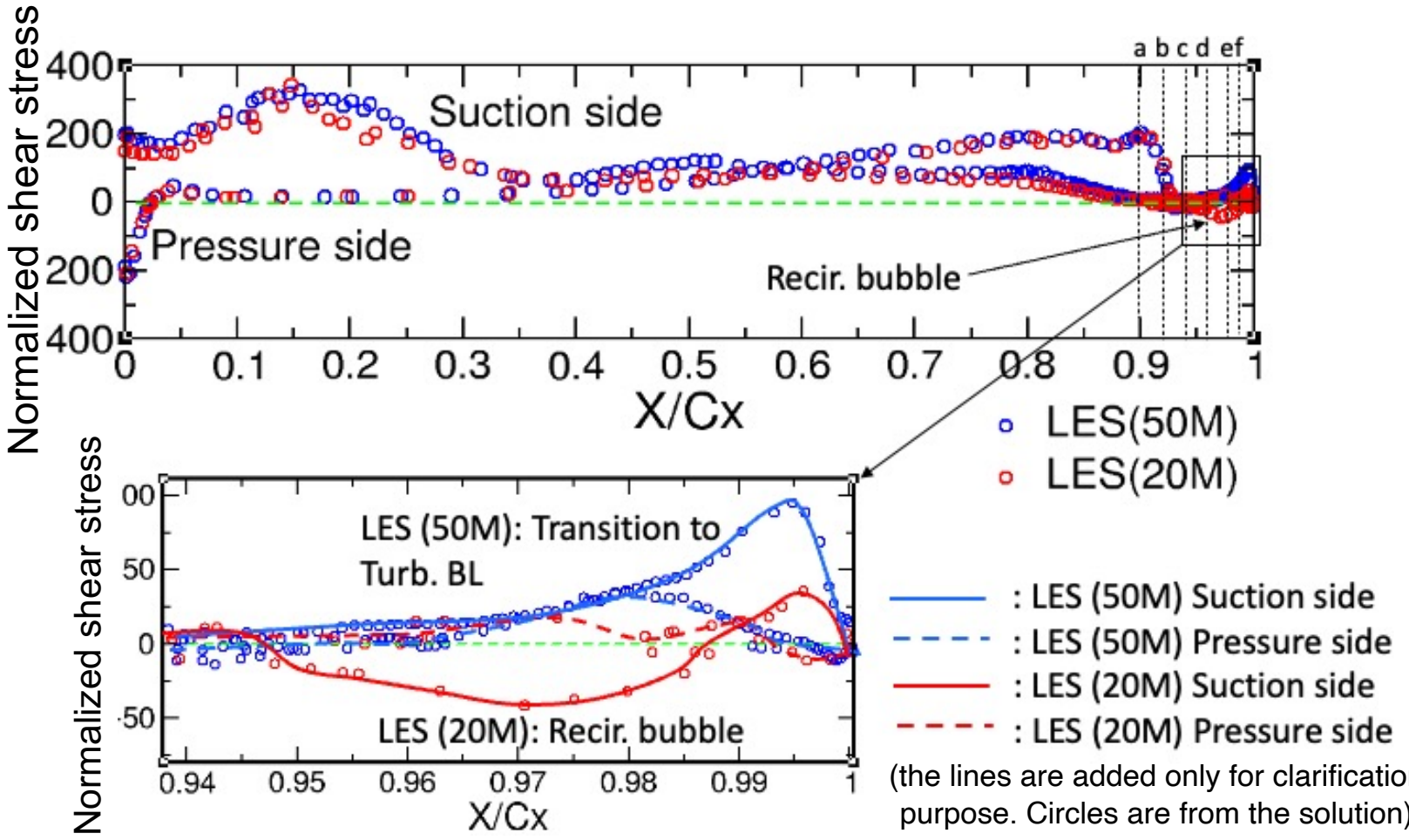
It is confirmed that the wake is spanwise uniform, and it suggests that an increase of the domain in the span direction is unnecessary.

Unresolved Turbulent Kinetic Energy (TKE)



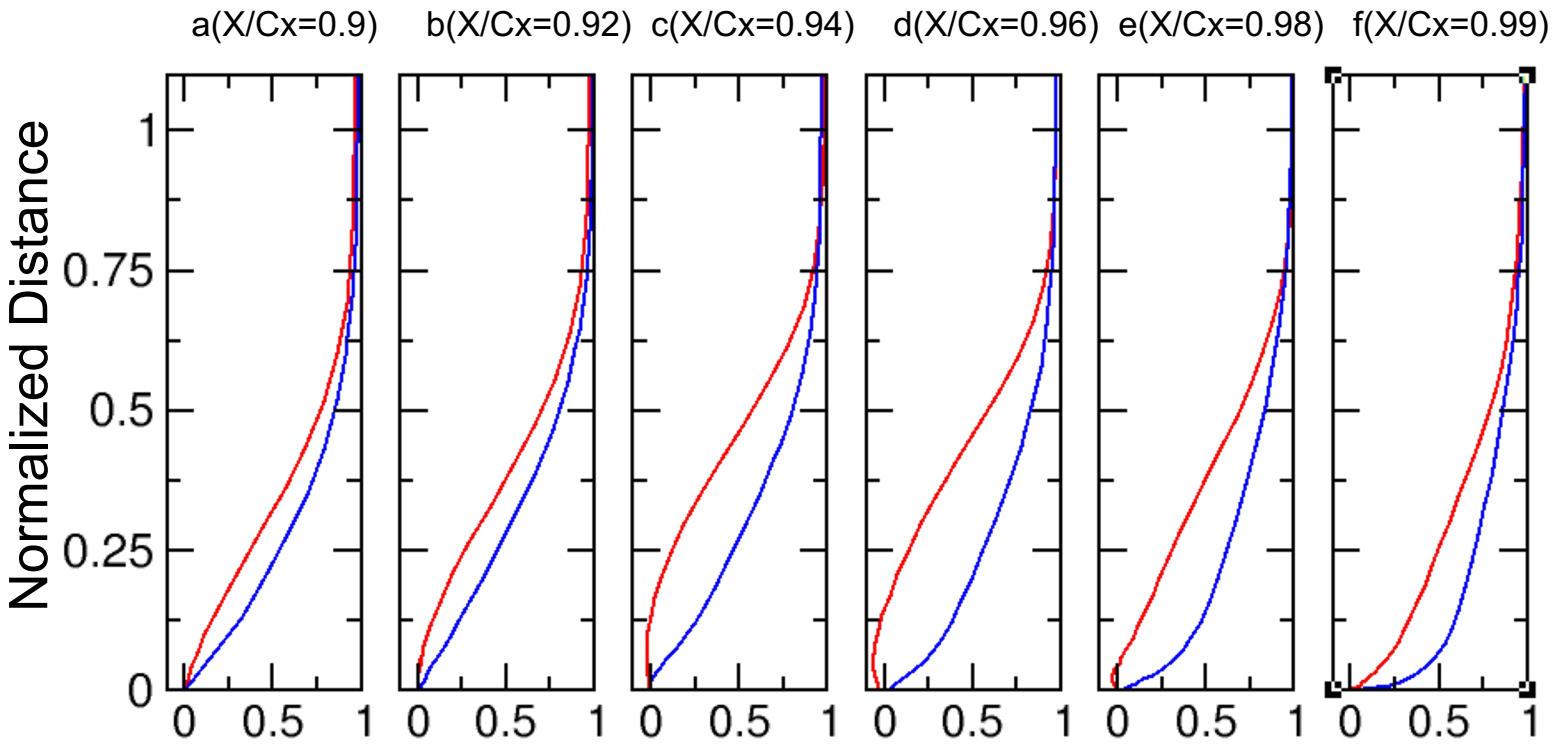
- Using LES (20M) mesh, a stable laminar boundary layer is formed and then, a thick and wavy boundary layer edge develops.
- Using LES (50M) mesh, the turbulent motions are resolved further (i.e., unresolved TKE diminishes). It looks like that the boundary layer appears to have transitioned into a turbulent boundary layer indicated by sudden increase of TKE.

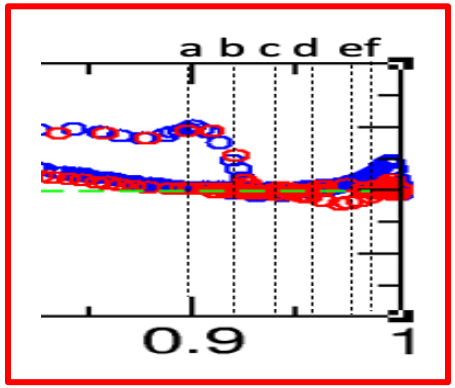
Shear Stress Profile



- Both cases show very similar shear profiles except the end of the suction side.
- LES (20M) mesh shows zero shear stress (from X/C_x=0.9 to X/C_x =0.94), indicating that flow is about to separate, and then the recirculation bubble is formed.
- LES (50M) mesh shows the shear stress remains positive and rapidly increases around X/C_x =0.96, where the transition to the boundary layer takes place.

Boundary Layer Profile



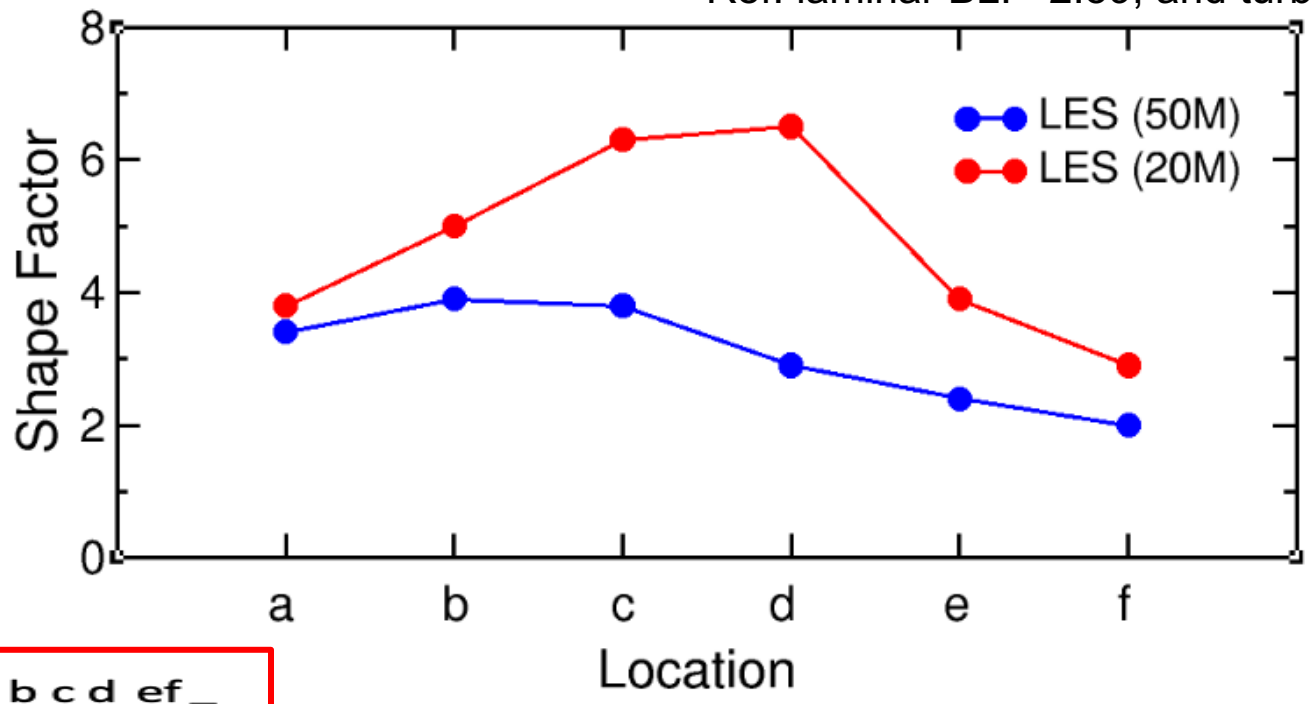


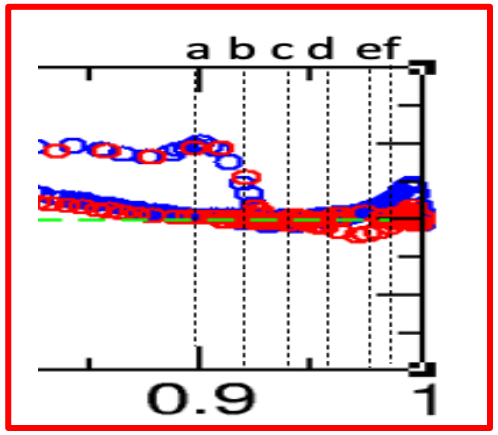
Suction side close to the trailing edge

- Using LES (50M) mesh, the BL appears fuller due to more momentum transfer from the freestream turbulence and production of TKE inside the boundary layer more.
- In [8], the time-averaged shear stress and the pressure loading profiles did not indicate a small recirculation bubble → More demanding mesh requirement when modeling this type of blade with large trailing edge diameter.

Shape Factor

Ref: laminar BL: ~2.59, and turbulent BL: ~1.3

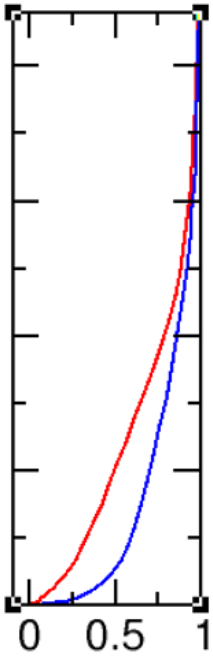




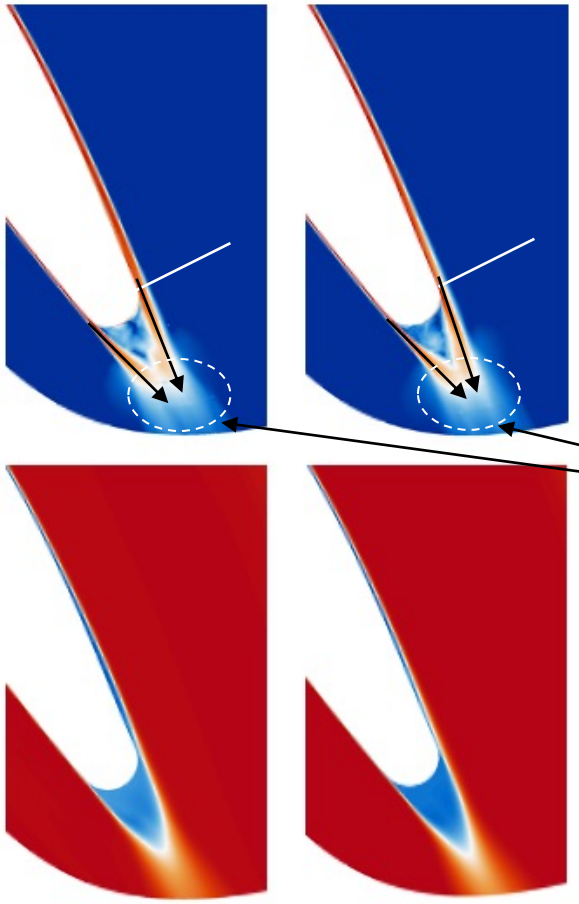
Suction side close to the trailing edge

- Both meshes shows the same characteristic of the BL at point a (X/Cx=0.9) and then the shape factors diverse significantly.
- For the LES (50M), the shape factor smoothly starts decreasing (***a faster momentum thickness growth means a stronger turbulent dissipation***), indicating that the boundary layer is transferring into the turbulent boundary layer.

Time-Averaged Dissipation Function and Angle



Velocity profile at the edge
(along white line)



Log(Diss. func.)

1000

0.1

$$\Phi = \frac{\mu}{2}\left(\frac{\partial u_i}{\partial x_j} + \frac{\partial u_j}{\partial x_i}\right)^2 - \frac{2\mu}{3}\left(\frac{\partial u_i}{\partial x_i}\right)^2$$

Dissipation function

Pt

1.0

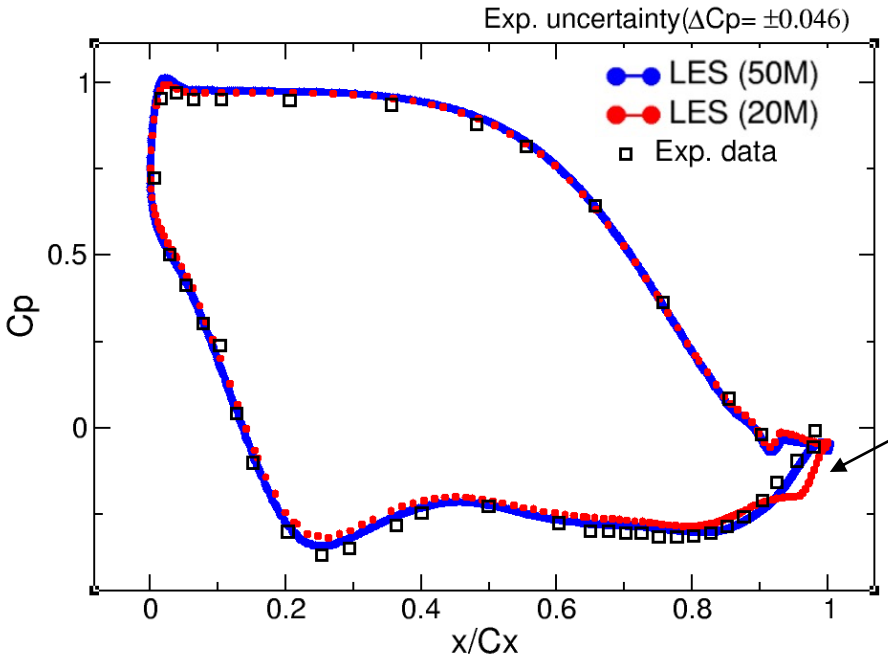
0.6

These angles are sightly changed.

- The dissipation function appears in the entropy transport equation and is related to the loss process. Both meshes predict similar profile of dissipation function and total pressure. However, LES (20M) mesh shows larger boundary layer loss (i.e., thicker red zone)
- The thicker boundary layer predicted by using the LES (20M) mesh causes the point, where two boundary layers from the pressure and suction sides meet, to be shifted upward.

Compared with the Experimental Data

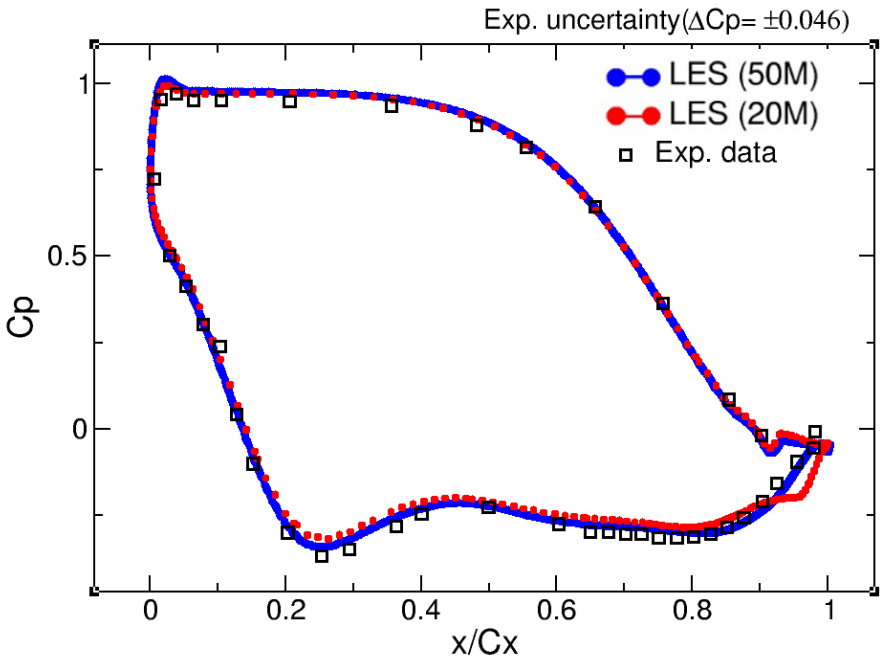
Midspan Blade Loading



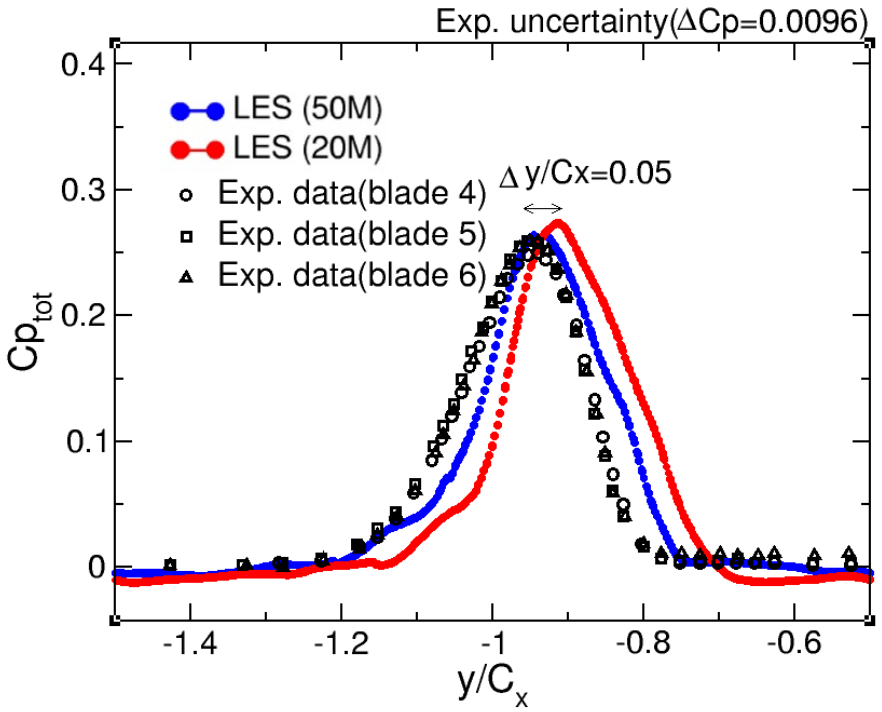
When using the LES (50M), there is no kink associated with the separation bubble at X/C_x = 0.95

Compared with the Experimental Data

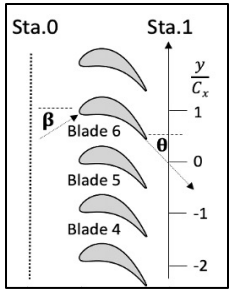
Midspan Blade Loading



Wake Profile



- The predicted profile (LES (50M)) gets close to the data (i.e., less shifted), and thus the peak location matches the data within the experimental uncertainty.
- The area-averaged kinetic energy loss coefficients, are, 0.0438 for LES (20M) and 0.0414 for LES (50M), and very close to the measured data (=0.042).



Conclusions

We utilized Large eddy simulation to calculate the pressure loading profile, the total loss distribution, and the integrated pressure loading profile of the front-loaded CMC blade at the high-freestream turbulence (*Tu*=13%).

Key Observations

- In our previous studies [8], we reported the issues (a small recirculation bubble at the end of the suction side and the ``shifted'' wake profile), which are resolved by local grid refinement at the trailing edge and expanding the span.
- With the new mesh, there is no recirculation bubble observed due to the fact the boundary layer is energized more from the momentum transfer from the free stream turbulence.
- The transition to the turbulent boundary layer (bypass transition) was observed (not separation reattachment previously reported [8])
- The increase in the span of the blade seem to have no noticeable effect on the solution.
- The fuller velocity profile alters the direction of the shear layer departing from the trailing edge, which reduces the shift of the wake profile.

Reference

[1] Giel, P., Shyam, V., Juangphanich, P., and Clark, J.P., 2020, “Effects of Trailing Edge Thickness and Blade Loading Distribution on the Aerodynamic Performance of Simulated CMC Turbine Blades,” Proceedings of the ASME Turbo Expo, Virtual, GT2020-15802.

[2] Lyall, M. E., King, P., Sondergaard, R. S., and Clark, J., 2012, “An Investigation of Reynolds Lapse Rate for Highly Loaded Low Pressure Turbine Airfoils With Forward and Aft Loading,” Journal of Turbomachinery: 134, p. 051035-1.

[3] Keadle, K., and McQuilling, M., 2013, “Evaluation of RANS Transition Modeling for High Lift LPT Flows at Low Reynolds Number,” Proceedings of the ASME Turbo Expo, Virtual, San Antonio, TX, USA, June 20013, GT2013-95069.

[4] Arko-, B., and McQuilling, M., 2013, “Computational Study of High-Lift Low-Pressure Turbine Cascade Aerodynamics at Low Reynolds Number,” Journal of Propulsion and Power: 29, 446-459

[5] Medic, G., Sharma, O., 2012, “Large-Eddy Simulation of Flow in a Low-Pressure Turbine Cascade,” Proceedings of the ASME Turbo Expo, Copenhagen, Denmark, June 2012, GT2012-68878

[6] Bolinches-Gisbert, M., Robles, D.C., Corral, R., and Gisbert., 2020, “Prediction of Reynolds Number Effects on Low-Pressure Turbines Using a High-Order ILES Method,” Journal of Turbomachinery: 142, p 031002.

[7] Pichler, R., Sandberg, R.D., Michelassi, V., “Assessment of Grid Resolution Requirements for Accurate Simulation of Disparate Scales of Turbulent Flow in Low-Pressure Turbines,” Proceedings of the ASME Turbo Expo, GT2016-56858

[8] Miki, K., Ameri, A., 2022, “Numerical Investigation of the Effect of Trailing Edge Thickness of Simulated CMC Blades on Loss Profiles ,” Proceedings of the ASME Turbo Expo, Rotterdam, Netherlands, June 2022, GT2022-82335

[9] Klein, M., Sadiki, A., Janicka, J., 2003, “A Digital Filter Based Generation of Inflow Data for Spatially Developing Direct Numerical or Large Eddy Simulations", Journal of Computational Physics: 186, 652-665.

[10] Kim, W.-W. Menon, S., 1995, “A New Dynamic One-equation Subgrid-scale Model for Large Eddy Simulations," Proceedings of the 33rd AIAA Aerospace Sciences Meeting and Exhibit, January 1995, AIAA Paper 1995-356.

[11] Liou, M.-S., 2006, “A Sequel to AUSM, Part II: AUSM+-up for All Speeds," Journal of Computational Physics: 214, p 137-170.

[12] Miki, K., Ameri, A., 2021, “Improved Prediction of Losses with Large Eddy Simulation in a Low-Pressure Turbine,” Journal of Turbomachinery, (in print), TURBO-21-1207 doi.org/10.1115/1.4053234.

[13] Thurman, D., Flegel, A., Giel, Pau., 2014, “Inlet Turbulence and Length Scale measurements in a Large-Scale Transonic Turbine Cascade,” Proceedings of the 50th AIAA Joint Propulsion Conference, AIAA 2014-3934



Thank you!

Questions?

Acknowledgement

- **Supported by NASA HyTech Project (Project manager, Dr. Evans, Laura)**
- **Simulations conducted NASA Advanced Supercomputing (NAS) Pleiades computers**
- **Grid Generation conducted with GridPro**
- **Flow Viz was conducted with FieldView**